Accordingly, the performance curve for the H^{++} group in Fig. 4A may underestimate the deficit. The H^{++} monkeys were as impaired as H^+A^+ monkeys on a second task, retention of object discriminations (68.4% versus 69.5% correct, respectively, averaged across four discriminations, each tested on three different days).
38. S. Zola-Morgan *et al.*, *J. Neurosci.* **9**, 4355 (1989).
39. We propose that effects on memory reported in previous studies with A^+ lesions are due to damage to perirhinal cortex that necessarily occurs during the surgical approach to the amygdala [R. C. Saunders, E. A. Murray, M. Mishkin, *Neuropsychologia* **22**, 785 (1984); E. Murray and M. Mishkin, *J. Neurosci.* **6**, 1991 (1986); or the amygdalofugal pathway [J. Bachevalier, J. K. Parkinson, M. Mishkin, *Exp. Brain Res.* **57**, 554 (1985)]. See also (*11*). For a similar interpretation of the earlier work, see [E. Murray, in *The Amygdala*, J. Aggleton, Ed. (Wiley, New York, in press)].
40. M. Davis, *Behav. Neurosci.* **100**, 814 (1986); D. Gaffan and S. Harrison, *J. Neurosci.* **7**, 2285 (1987); J. E. LeDoux, in *Handbook of Physiology: The Nervous System V. Higher Functions of the Nervous System*, J. M. Brookhart and V. B. Mountcastle, Eds. (American Physiological Society, Bethesda, MD, 1987), vol. 5, pp. 419–460; M. Gallagher *et al.*, *J. Neurosci.* **10**, 1906 (1990); R. P. Kesner, in *The Amygdala*, J. Aggleton, Ed. (Wiley, New York, in press).
41. E. A. Murray and M. Mishkin, *Science* **228**, 604 (1985).
42. S. Zola-Morgan *et al.*, *Hippocampus* **1**, 207 (1991).
43. These include pioneering studies of cooling the temporal cortex in monkeys [J. A. Horel and D. E. Pytko, *J. Neurophysiol.* **47**, 11 (1982); J. A. Horel and D. E. Pytko-Joiner, M. Voytko, K. Salsbury, *Behav. Brain Res.* **23**, 29 (1987)], studies of local cerebral glucose utilization in monkeys during the performance of memory tasks [H. R. Friedman and P. S. Goldman-Rakic, *J. Neurosci.* **8**, 4693 (1988)], studies of normal human memory with positron emission tomography [L. R. Squire *et al.*, *Soc. Neurosci. Abstr.*, in press], and neuropsychological studies of cognitive impairment [H. Damasio and A. R. Damasio, *Lesion Analysis in Neuropsychology* (Oxford Univ. Press, New York, 1989)].
44. M. Mishkin, *Philos. Trans. R. Soc. London B* **298**, 85 (1982).
45. J. P. Aggleton and M. Mishkin, *Exp. Brain Res.* **58**, 190 (1985); J. Bachevalier, R. Saunders, M. Mishkin, *ibid.* **57**, 547 (1985).
46. Medial thalamic lesions in monkeys and humans can produce severe memory impairment [M. Victor, R. D. Adams, G. H. Collins, *The Wernicke-Korsakoff Syndrome* (Davis, Philadelphia, ed. 2, 1989); J. P. Aggleton and M. Mishkin, *Neuropsychologia* **21**, 189 (1983); D. Y. von Cramon, N. Hebel, U. Schuri, *Brain* **108**, 993 (1985); N. R. Graff-Radford, D. Tranel, G. W. Van Hoesen, J. Brandt, *ibid.* **113**, 1 (1990)], perhaps by virtue of the projections to the medial thalamus that originate in the hippocampus as well as in entorhinal cortex and perirhinal cortex [D. G. Amaral, in *Handbook of Physiology: The Nervous System: Higher Functions of the Nervous System*, J. M. Brookhart and V. B. Mountcastle, Eds. (American Physiological Society, Bethesda, MD, 1987), vol. 5, pp. 211–294]. Enduring memory impairment can also occur after damage to the cholinergic basal forebrain [A. R. Damasio, N. R. Graff-Radford, P. J. Eslinger, H. Damasio, N. Kassell, *Arch. Neurol.* **42**, 263 (1985)], which has strong anatomical connections to medial temporal lobe structures [M.-M. Mesulam, E. J. Mufson, A. I. Levy, B. H. Wainer, *J. Comp. Neurol.* **214**, 170 (1983)].
47. P. Alvarez-Royo, R. Clower, S. Zola-Morgan, L. R. Squire, *J. Neurosci. Methods*, in press; R. Clower, P. Alvarez-Royo, S. Zola-Morgan, L. R. Squire, *Soc. Neurosci. Abstr.*, in press.
48. Results from rodents are similar to the findings from H and H^+ monkeys in that damage involving the hippocampus proper plus the subiculum produced more memory impairment than damage limited to the hippocampus [L. E. Jarrard, in *The Hippocampus*, R. L. Isaacson and K. H. Pribram, Eds. (Plenum, New York, 1986), vol. 4, pp. 93–126; R. G. M. Morris, F. Schenk, F. Tweedie, L. E. Jarrard, *Eur. J. Neurosci.* **2**, 1016 (1990)].
49. S. Zola-Morgan *et al.*, *Soc. Neurosci. Abstr.* **15**, 341 (1989); S. Zola-Morgan and L. R. Squire, in *The Biology of Memory*, L. R. Squire and E. Lindenlaub, Eds. (Schattauer Verlag, Stuttgart, 1990), pp. 509–521; N. Rempel, R. Clower, D. G. Amaral, S. Zola-Morgan, L. R. Squire, *Soc. Neurosci. Abstr.*, in press. Global ischemia was produced by 15 min of bilateral carotid occlusion together with pharmacologically induced hypotension.
50. H. P. Davis and B. Volpe, in *The Biology of Memory*, L. R. Squire and E. Lindenlaub, Eds. (Schattauer Verlag, Stuttgart, 1990), pp. 477–504.
51. L. R. Squire, *Memory and Brain* (Oxford Univ. Press, New York, 1987); A. R. Damasio, *Cognition* **33**, 25 (1989); W. Singer, *Concepts Neurosci.* **1**, 1 (1990).
52. L. R. Squire, A. P. Shimamura, D. G. Amaral, in *Neural Models of Plasticity*, J. Byrne and W. Berry, Eds. (Academic Press, New York, 1989), pp. 208–239.
53. D. Marr, *Philos. Trans. R. Soc. London B* **176**, 23 (1971); B. McNaughton and L. Nadel, in *Neuroscience and Connectionist Theory*, M. Gluck and D. Rumelhart, Eds. (Erlbaum, Hillsdale, NJ, 1990), pp. 1–63.
54. T. V. P. Bliss and T. Lomo, *J. Physiol. (London)* **232**, 331 (1973).
55. S. Zola-Morgan and L. R. Squire, *Science* **250**, 288 (1990).
56. L. R. Squire *et al.*, *Behav. Neurosci.* **102**, 210 (1988); J. P. Aggleton *et al.*, *Neuropsychologia* **26**, 265 (1988).
57. D. P. Salmon, S. Zola-Morgan, L. R. Squire, *Psychobiology* **15**, 37 (1987).
58. B. L. Malamut, R. C. Saunders, M. Mishkin, *Behav. Neurosci.* **98**, 759 (1984).
59. W. H. Overman, G. Ormsby, M. Mishkin, *Exp. Brain Res.* **79**, 18 (1990).
60. Skills and habits may depend on the neostriatum [M Packard, R. Hirsch, N. White, *J. Neurosci.* **9**, 1465 (1989); J. Wang, T. Aigner, M. Mishkin, *Soc. Neurosci. Abstr.* **16**, 617 (1990); J. Saint-Cyr, A. Taylor, A. Lang, *Brain* **111**, 941 (1988); W. Heindel, D. Salmon, C. Shults, P. Walicke, N. Butters, *J. Neurosci.* **9**, 582 (1989)]. For information about the neural substrates of other kinds of nondeclarative memory, see (*40*). Also see E. Tulving and D. Schacter, *Science* **247**, 385 (1990); L. R. Squire *et al.*, *Soc. Neurosci. Abstr.*, in press; R. F. Thompson, *Science* **233**, 941 (1986); M. Davis, T. Parsi, D. Gendelman, M. Tischler, J. Kehne, *ibid.* **218**, 688 (1982); R. Leaton and W. Supple, Jr., *ibid.* **232**, 513 (1986).
61. L. R. Squire, in *The Biology of Memory*, L. R. Squire and E. Lindenlaub, Eds. (Schattauer Verlag, Stuggart, 1990), pp. 643–664.
62. We thank D. Amaral, P. Alverez-Royo, R. Clower, N. Remple, and W. Suzuki for their contributions to the work summarized here. Supported by the Medical Research Service of the Department of Veterans Affairs, the Office of Naval Research, NIH grant NS19063, NIMH grant MH24600, and the McKnight Foundation.

Research Article

Reexamination of the Folding of BPTI: Predominance of Native Intermediates

JONATHAN S. WEISSMAN AND PETER S. KIM

Bovine pancreatic trypsin inhibitor (BPTI) continues to be the only protein for which a detailed pathway of folding has been described. Previous studies led to the conclusion that nonnative states are well populated in the oxidative folding of BPTI. This conclusion has broadly influenced efforts to understand protein folding. The population of intermediates present during the folding of BPTI has been reexamined by modern separation techniques. It was found that all well-populated folding intermediates contain only native disulfide bonds. These data emphasize the importance of native protein structure for understanding protein folding.

EFFORTS TO UNDERSTAND PROTEIN FOLDING ARE HAMpered by the transient nature of kinetic folding intermediates. In a series of pioneering studies (*1, 2*) begun in the mid-1970s, this difficulty was circumvented by trapping disulfide-bonded folding intermediates, and the folding pathway of bovine pancreatic trypsin inhibitor (BPTI) was described in terms of the intermediates that accumulate substantially during folding. Native BPTI (N) contains three disulfide bonds (Fig. 1), indicated by the cysteines involved (*3*) as [30-51; 5-55; 14-38]. The protein unfolds on reduction of these disulfide bonds, even in the absence of denaturants. Although there are 75 possible species of BPTI con-

The authors are in the Howard Hughes Medical Institute, Whitehead Institute for Biomedical Research, 9 Cambridge Center, Cambridge, MA 02142. In addition, J. S. Weissman is in the Department of Physics and P. S. Kim is in the Department of Biology, Massachusetts Institute of Technology, Cambridge, MA.

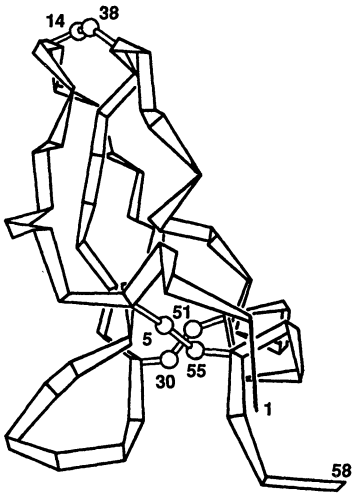

Fig. 1. A schematic diagram of native BPTI with its three disulfide bonds. [Adapted from (*9*)]

taining one or more disulfide bonds, only eight (including native BPTI) appeared to accumulate significantly during folding. These studies provided important experimental evidence indicating that the number of states sampled in protein folding reactions is restricted before folding is complete.

The striking and counter-intuitive result in those studies, however, was that three of the well-populated species contain disulfide bonds not present in the native protein. Moreover, in the kinetically preferred route for folding deduced from those studies (*1, 4*), folding proceeds through either of two well-populated intermediates that contain nonnative disulfide bonds, [30-51; 5-14] and [30-51; 5-38]. The finding that nonnative interactions appear to stabilize substantially some folding intermediates complicates significantly efforts to understand the folding process.

We have taken advantage of improvements that have been made in separation technologies since the original BPTI folding experiments (*5*) to reexamine the spectrum and population of intermediates present during the oxidative folding of BPTI. Six species accumulate to significant levels: [5-55], [30-51], [30-51; 14-38], [30-51; 5-55], [5-55; 14-38] and native (N). All of these species contain only disulfide bonds that are present in native BPTI.

As in earlier studies (*4*), the folding of BPTI is found to occur via disulfide bond rearrangement as opposed to direct oxidation. The rearrangement, however, is a relatively random process and does not appear to be directed by specific nonnative intermediates. Rather, the rate-limiting step in the rearrangement involves the loss of native structure.

Identification of disulfide intermediates. In the earlier studies, folding of reduced BPTI (R) was initiated by the addition of an oxidizing agent. At various time points, folding was stopped by addition of iodoacetate, a reagent that alkylates free thiols and thereby prevents further oxidation or thiol-disulfide exchange. After separation of the trapped intermediates by ion-exchange chromatography (IEC), the disulfide linkages of the intermediates were determined by two-dimensional paper electrophoresis (*6*).

In our studies, a rapid and sensitive method for identifying disulfide bonds in an intermediate was developed. Starting with a purified intermediate, in which the thiols of cysteine residues that were not disulfide-bonded had been blocked previously with iodoacetate, we used the following method (*7*). (i) The disulfide bonds in the intermediate were reduced; (ii) the resultant thiols were labeled with a fluorescent iodoacetate derivative, IAEDANS; (iii) the protein was digested with thermolysin; (iv) labeled fragments (indicating Cys residues that were originally involved in disulfide bonds) were identified by reversed-phase high-performance liquid chromatography (HPLC) (Fig. 2).

In the above identification scheme, digestion with thermolysin was always carried out on a fully reduced species. Consequently, cleavage proceeds to a similar extent for all intermediates. This provides a sensitive check for purity (Fig. 2). One limitation of this method that can be overcome by straightforward modifications (*8*) is that the pairwise linkages of disulfide bonds are not identified. For example, the intermediates [30-51; 5-55], [30-55; 5-51] and [30-5; 51-55] are not distinguished. Almost all of the two-disulfide intermediates that were identified in our study, however, had also been identified by paper electrophoresis (*9*), which does give pairwise linkages. Our disulfide bond assignments are based on these pairwise linkages.

Incomplete chromatographic resolution of intermediates. The IEC chromatogram for a 3-minute BPTI folding time point (*10*) is shown in Fig. 3A. Individual IEC peaks were collected and

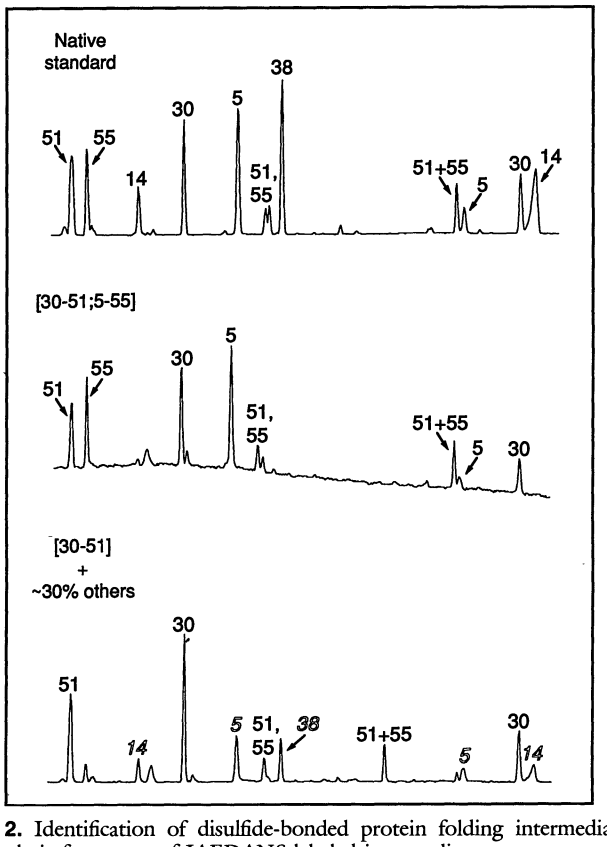

Fig. 2. Identification of disulfide-bonded protein folding intermediates. Proteolytic fragments of IAEDANS-labeled intermediates are separated by HPLC. Numbers above the peaks denote the labeled cysteines contained in the fragments. In order to illustrate how the method provides a sensitive check for purity, contaminants (about 30 percent) were added to a pure sample of [30-51]. These impurities are indicated by the small amounts of labeled Cys^5, Cys^{14}, and Cys^{38}. In the "Native Standard" chromatogram, the sequences of the labeled peaks, from left to right, are (labeled cysteine residue numbers are given in parentheses): AEDC(51), TC(55)GGA, TGPC(14)K, LC(30)QT, FC(5), AEDC(51)MR + MRTC(55)GGA, VYGGC(38)R, AEDC(51)MRTC(55)GGA, RPDFC(5), LC(30)QTF, and LEPPYTGPC (14)K. The fragment containing Cys^{51} and Cys^{55} elutes earlier in the gradient in the identification of [30-51] than does the fragment with the same amino acid sequence in the native standard and in the identification of [30-51; 5-55]. This is due to the presence of only one IAEDANS molecule (at Cys^{51}) in this fragment as compared to two (at Cys^{51} and Cys^{55}) in the native standard and in [30-51; 5-55]. Two numbers separated by a comma indicate that two fragments elute at that position. The peak denoted 51 + 55 contains a fragment with both Cys^{51} and Cys^{55}. IAEDANS is *N*-iodoacetyl-*N'*-(5-sulfo-1-naphthyl)ethylenediamine. Abbreviations for the amino acid residues are: A, Ala; C, Cys; D, Asp; E, Glu; F, Phe; G, Gly; H, His; I, Ile; K, Lys; L, Leu; M, Met; N, Asn; P, Pro; Q, Gln; R, Arg; S, Ser; T, Thr; V, Val; W, Trp; Y, Tyr.

analyzed further by HPLC. Several of the HPLC peaks were identified by the IAEDANS method, and are so marked (Fig. 3B). Both of the one-disulfide IEC peaks, assigned previously as (30-51) and (5-30), contained substantial impurities as determined by HPLC (Fig. 3B). Significantly, [5-55] was one of the contaminating species in the (30-51) peak (*3*). The native intermediate [5-55] had not been detected previously although its existence had been inferred from kinetic folding experiments (*2*), and from studies of peptide (*11*) and recombinant (*12, 13*) models.

The two-disulfide IEC peaks assigned in earlier studies as (30-51; 5-55), also known as N_{SH}^{SH} (*14*), and (30-51; 14-38) were relatively pure as indicated by HPLC. The IEC peak known to contain both native BPTI (N) and a quasi-native species [5-55; 14-38], denoted N* (*15*), was also virtually free of impurities (Fig. 3B). These species all contained only native disulfide bonds. Furthermore, two of these intermediates (N_{SH}^{SH} and N*) are known to be completely folded in a native conformation (*14, 15*).

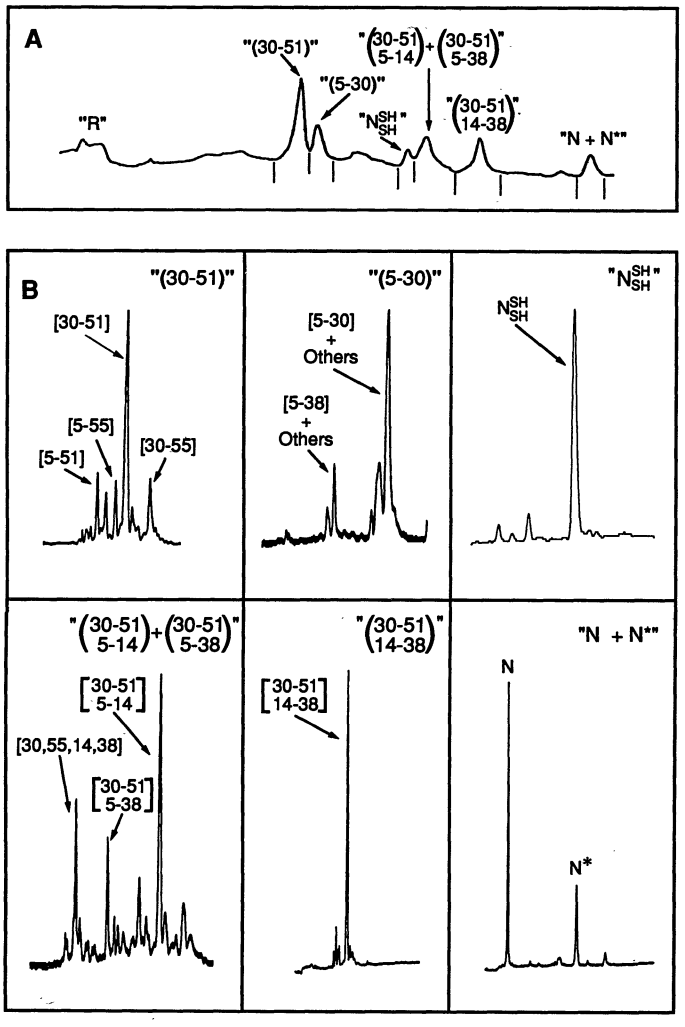

Fig. 3. HPLC analysis of trapped BPTI folding intermediates obtained by ion-exchange chromatography (*10*). The folding of BPTI was allowed to proceed for 3 minutes and then quenched with iodoacetate; the mixture was fractionated by ion-exchange chromatography (IEC). (**A**) The IEC elution profile, monitoring absorbance at 280 nm, is similar to that reported earlier (*9*). (**B**) Reversed-phase HPLC analysis of the IEC fractions, pooled as indicated by lines in (A), monitoring absorbance at 229 nm. The disulfide bond linkages for the species indicated as [30, 55, 14, 38] have not been determined. All identified HPLC peaks are judged to be >85 percent pure, except for [5-30] and [5-38], which contain about 30 percent contaminants as judged by IAEDANS identification of disulfides (Fig. 2) and CZE. The peaks denoted N, N*, and [30-51; 14-38] are sharper because the HPLC gradient is steeper at the times when they elute.

In contrast, the IEC peak identified as containing the nonnative, two-disulfide intermediates, (30-51; 5-14) and (30-51; 5-38), was contaminated with several other species (Fig. 3B). This finding is noteworthy since (30-51; 5-14) and (30-51; 5-38) are the nonnative, two-disulfide intermediates thought to play an important role in the folding pathway for BPTI (*1*).

Disulfide rearrangements during quenching with iodoacetate. Alkylation of thiols by iodoacetate can distort the spectrum of intermediates present. This is demonstrated by the observation that there is an increase in the relative abundance of the native intermediate [30-51; 14-38] as the concentration of alkylating reagent is increased (Fig. 4A).

The fidelity of the iodoacetate quench was tested previously by alkylating with a different reagent (iodoacetamide) and by quenching with acid (*16*). The three quenching procedures gave a qualitatively similar distribution of single disulfides, as judged by polyacrylamide gel electrophoresis (PAGE). The initial two-disulfide intermediates, however, were not detected when acid quenching was used. The absence of these intermediates was attributed to intramolecular disulfide rearrangements, during the PAGE separation, to the native intermediate N_{SH}^{SH} (*17*). At the pH used in the PAGE separation, however, at least one of the missing intermediates, [30-51; 14-38], is stable for days (*18*). One possible alternative explanation is that [30-51; 14-38] coeluted with N by PAGE. This explanation is supported by the observation that [30-51; 14-38] coelutes with N by capillary zone electrophoresis (CZE) under similar conditions (*18*).

The observed rearrangements of intermediates during quenching with iodoacetate is not unreasonable since thiol-disulfide exchange is expected to occur on the same time scale as alkylation by iodoacetate. For example, alkylation of thiols with 100 mM iodoacetate occurs with a half-time of about 1 second at pH 8 (*17*). By comparison, given a second-order rate constant for thiol-disulfide exchange of $\sim 20\ M^{-1}\ s^{-1}$ (*2*) and effective concentrations for cysteines in an unfolded protein of ~50 mM (*2, 19, 20*), thiol-disulfide rearrangements in unfolded BPTI are also expected to occur on the second time scale.

If all of the thiols in all of the intermediates were equally reactive, then iodoacetate should still provide an effective quench. Although the six cysteines in BPTI are equally reactive in the reduced state (*21*), steric hindrance in partially structured intermediates (*22*) would retard the rate of alkylation of some thiols. An extreme example of slow alkylation by iodoacetate occurs with N*, which must be denatured before the thiols of Cys^{30} and Cys^{51} can be blocked, and even then substantial rearrangements occur (*2*). In addition to steric hindrance, the reactivity of a thiol can be altered substantially by changes in its local electrostatic environment (*23*). Finally, partially alkylated intermediates are likely to be destabilized and thus susceptible to rearrangement.

Regardless of the reason, the results (Fig. 3A) show that blocking with even a large excess of iodoacetate can lead to the preferential loss of a native intermediate. It is also likely that iodoacetate-induced rearrangements of native intermediates would contribute to the apparent abundance of nonnative disulfide species. Difficulty with iodoacetate quenching of an intermediate present during the reduction of ribonuclease A has also been observed (*24*).

Acid quenching. Because the thiolate anion is the reactive species in thiol-disulfide exchange, it is possible to quench folding extremely rapidly by lowering the pH. Protonation is reversible, however, so that acid-quenched intermediates must be separated rapidly (and at low pH) or they will rearrange or oxidize further. Reversed-phase HPLC at pH 2 is well suited to separate acid-quenched intermediates. A typical HPLC run takes less than 10^4 seconds. Therefore, as long as rearrangements occur on a time

scale slower than 10^4 seconds at pH 2 or, all else being equal, 10^{-2} second at pH 8, there will not be significant rearrangements during the separation. In contrast, blocking with 100 mM iodoacetate takes approximately 1 second at pH 8 (*17*). Thus, it is possible in theory, by using acid quenching and HPLC, to study intermediates that rearrange 100 times too rapidly to be trapped accurately with 100 mM iodoacetate.

A practical advantage of acid quenching is that it is reversible. As a result, it is possible to purify an acid-quenched intermediate and subsequently to allow further rearrangement or folding to occur. This advantage will facilitate detailed analyses of folding.

Four experiments demonstrate the validity of our acid quenching experiments. First, the distribution of intermediates observed does not depend on the concentration of acid used to quench folding (Fig. 4B). Second, all peaks that we checked, including all of the identified intermediates, elute as single peaks when they are rechromatographed by HPLC (*25*). Third, when a random distribution of intermediates, produced by allowing disulfide rearrangements to occur in the presence of high concentrations of denaturant, is subjected to HPLC separation, a large number of well-populated peaks is observed (Fig. 4C). This rules out the formal possibility that the small number of intermediates observed in folding experiments is the result of fast rearrangements that occur during the HPLC separation. Finally, when a sample of the same random mixture of intermediates was kept on an HPLC column for two or three times the period of a typical separation, the resultant chromatogram is similar to that observed when the material is eluted directly (Fig. 4C). This demonstrates that acid-quenched intermediates, including those that are inherently unstable, can be recovered quantitatively by HPLC.

Nature of BPTI folding intermediates. Although iodoacetate quenching should be used cautiously, it seems likely that higher concentrations of iodoacetate will provide a more accurate quench. When the folding of BPTI is studied with a more concentrated (500 mM) iodoacetate quench and the intermediates are quantitated by HPLC, the most abundant intermediates, at both the one- and two-disulfide stages, contain only native disulfide bonds (Fig. 5A). When the folding of BPTI is followed by an acid quench, the results are even more striking; all well-populated intermediates contain only native disulfide bonds (Fig. 5B). The most populated nonnative species, [30-51; 5-14], is almost ten times less populated than the corresponding native species, [30-51; 14-38].

The reversibility of acid quenching allowed us to examine part of the folding pathway of BPTI in detail. Acid-quenched [30-51; 14-38] was purified by HPLC. A rearrangement reaction was then initiated, in the absence of external oxidizing or reducing agents, by increasing the pH. Remarkably, populated intermediates are virtually absent during the rearrangement of [30-51; 14-38] to either of the other native two-disulfide intermediates, N_{SH}^{SH} or N* (Fig. 6A).

These results (Fig. 6A) suggest that the rate-limiting step (*26*) in the rearrangement is the loss of structure in [30-51; 14-38]. This conclusion contrasts with the suggestion that, as BPTI folds, structure is formed and broken rapidly in intermediates prior to the rate-limiting step, and that the rate-limiting step involves the formation of a distorted form of native-like conformation (*27*). Moreover, the extensive similarity to BPTI in patterns of two-dimensional nuclear magnetic resonance (2D-NMR) total correlation spectroscopy (TOCSY) cross-peaks (Fig. 7) suggests that [30-51; 14-38] is essentially completely folded (*28*). The extensive, native-like structure in [30-51; 14-38] is also almost certain to contribute to the difficulty observed in alkylating this intermediate.

Thus, [30-51; 14-38] acts as a kinetic trap with native-like structure. This conclusion predicts that denaturants, by destabilizing native structure, will increase the rate of folding. As the concentration of urea is increased from 0 to 6 M, the rate of rearrangement of [30-51; 14-38] to N_{SH}^{SH} and N* becomes approximately eight times higher (Fig. 6B), even though urea has little effect on the intrinsic rate of thiol-disulfide exchange (*29*). This result has little precedent in protein folding (see, however, *30, 31*), and earlier studies have shown that denaturants retard the overall rate of folding for BPTI

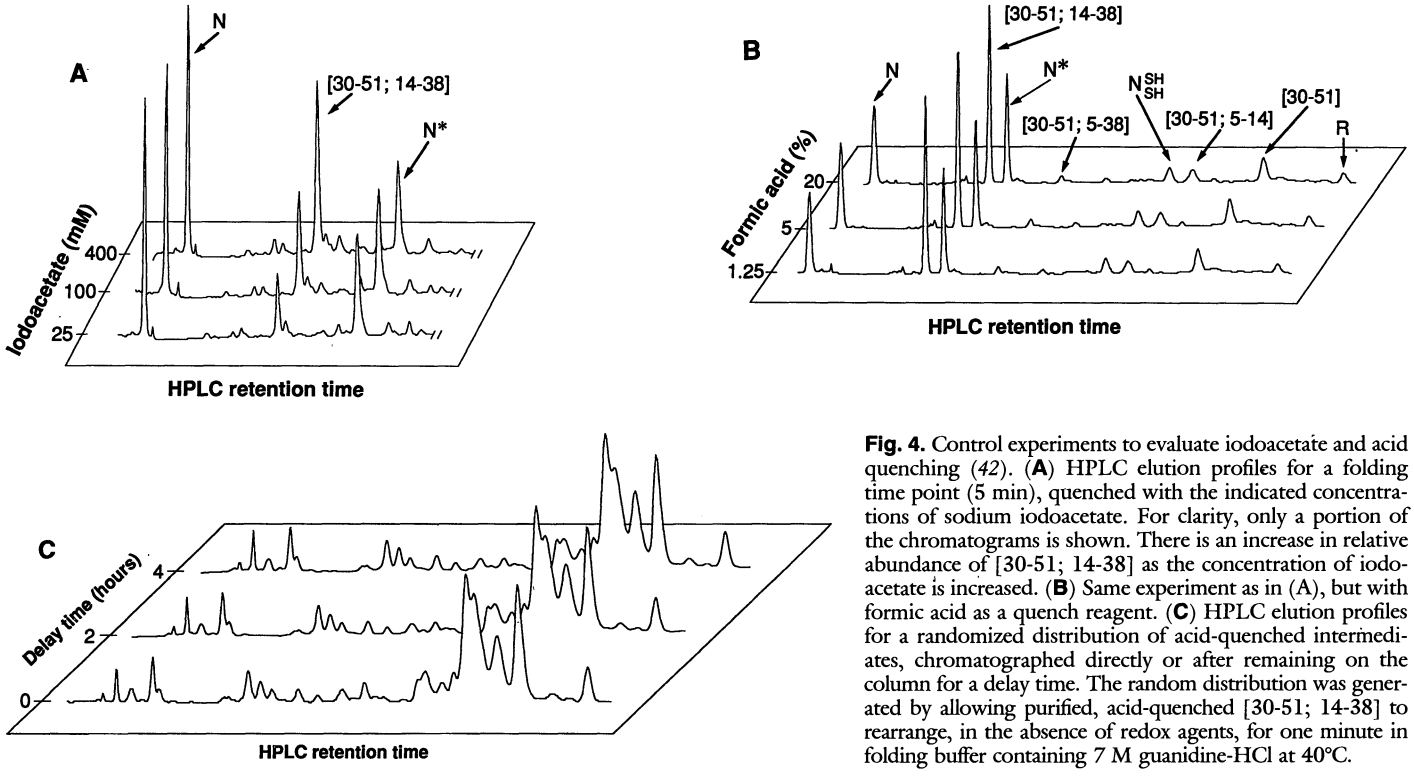

Fig. 4. Control experiments to evaluate iodoacetate and acid quenching (*42*). (**A**) HPLC elution profiles for a folding time point (5 min), quenched with the indicated concentrations of sodium iodoacetate. For clarity, only a portion of the chromatograms is shown. There is an increase in relative abundance of [30-51; 14-38] as the concentration of iodoacetate is increased. (**B**) Same experiment as in (A), but with formic acid as a quench reagent. (**C**) HPLC elution profiles for a randomized distribution of acid-quenched intermediates, chromatographed directly or after remaining on the column for a delay time. The random distribution was generated by allowing purified, acid-quenched [30-51; 14-38] to rearrange, in the absence of redox agents, for one minute in folding buffer containing 7 M guanidine-HCl at 40°C.

(*29, 32*). The ability to uncover a specific step in the folding reaction that is accelerated by denaturants illustrates the utility of acid-quenched intermediates for investigating protein folding.

The reversibility of acid quenching also made it possible to determine the equilibrium distribution of one-disulfide species. Acid-quenched [5-55] was purified by HPLC and then allowed to rearrange. The results (Fig. 8A) show that the predominant one-disulfide species is [30-51]. Essentially the same chromatogram was obtained when acid-quenched [30-51] was used as the starting material (Fig. 8A), indicating that equilibrium had been reached.

On the basis of 2D-NMR studies of a synthetic peptide model (called PαPβ), the native intermediate [30-51] is thought to contain native-like secondary and tertiary structure (*33*). Studies of iodoacetate-trapped (30-51) also indicate that β-sheet structure is present. Unlike studies of PαPβ, however, studies of (30-51) did not detect α-helical structure, nor did they indicate that there were significant native tertiary interactions (*34*). The most likely source for these differences is that iodoacetate-trapped (30-51) contains a bulky and charged modifying group at Cys^{55}, whereas this cysteine is replaced by alanine in the peptide model. This residue is part of the α helix and is involved in tertiary interactions with the β sheet (*33*), so that the carboxymethyl group is expected to interfere with folding.

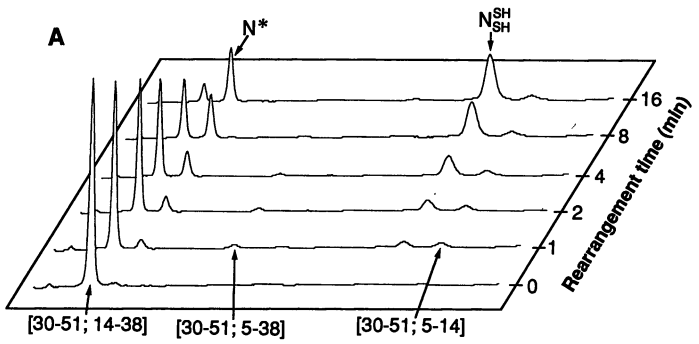

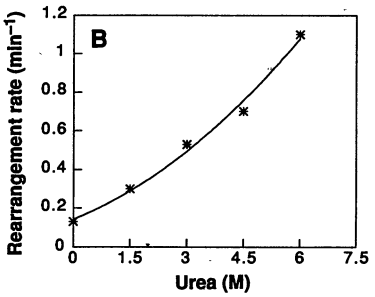

Fig. 6. Rearrangement of a purified protein folding intermediate (*45*). (**A**) Acid-quenched [30-51; 14-38], purified by HPLC, was allowed to rearrange by raising the pH to 8.7 in the absence of redox reagents and in anaerobic conditions. At the indicated times, a portion of the sample was quenched with acid (*44*) and analyzed by HPLC. (**B**) Urea dependence of the rate of rearrangement of [30-51; 14-38] (*46*).

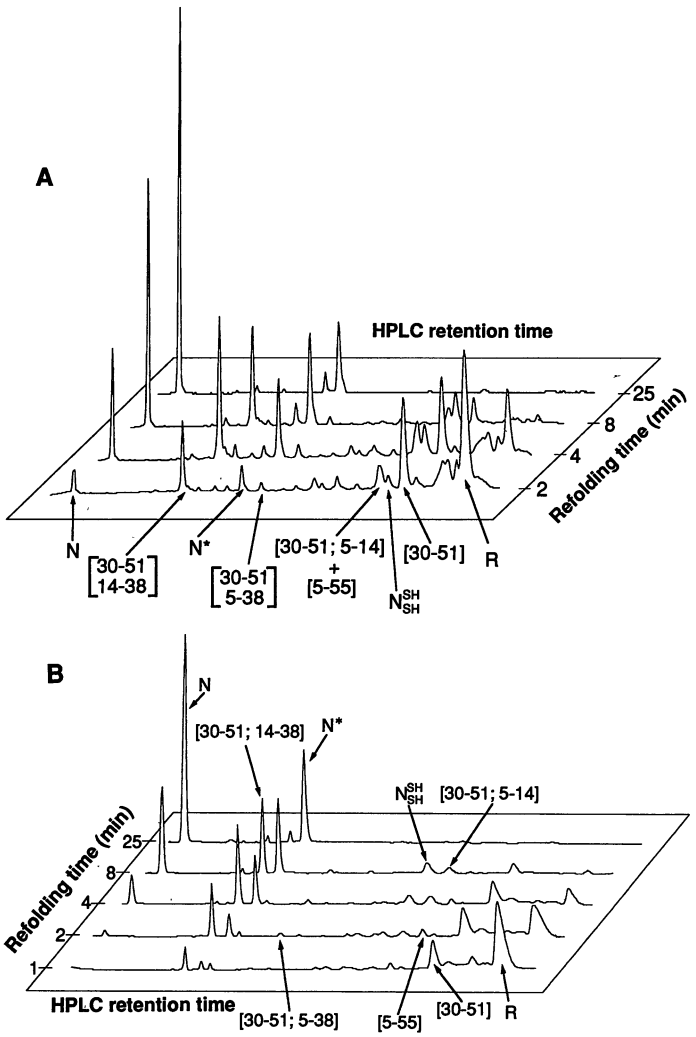

Fig. 5. HPLC chromatograms obtained after various times of folding (pH 8.7, 25°C, 150 μM oxidized glutathione). (**A**) Quenched with a high concentration (500 mM) of iodoacetate (*43*). (**B**) Quenched with 5 percent formic acid (*44*).

The native intermediate [5-55] is also present at equilibrium, but it is about seven times less populated than [30-51]. The remaining single disulfides appear to be spread over many other species. In contrast to earlier studies (*1, 19*), the nonnative intermediate [5-30] does not appear to have substantial stability.

Folding at neutral pH. Earlier studies of the folding of BPTI were performed at pH 8.7 in order to effect a rapid rate of thiol-disulfide exchange without significantly deprotonating the tyrosine residues (*1*). The pK_a values for Cys thiols are near 8.7, however, so that there is a heterogeneous population of intermediates, with different ionization states at different cysteine residues, for a given disulfide linkage at pH 8.7. In addition, structure in intermediates can alter the pK_a of the cysteines. Therefore, results obtained at neutral pH should simplify interpretation of the structural basis of the folding pathway.

For this reason, the folding of BPTI at pH 7.3, but otherwise identical conditions, was examined (Fig. 9). The relative abundance of [5-55] increases at neutral pH, so that it is the predominant one disulfide intermediate. The marked increase in the abundance of [5-55] as the pH is lowered results most likely from removing the destabilizing effect of burying deprotonated (that is, negatively charged) thiols at Cys^{30} and Cys^{51} in this intermediate. Equilibrium experiments (Fig. 8B) demonstrate that the abundance of [5-55] at neutral pH reflects the thermodynamic stability of this intermediate.

Structural studies indicate that native structure contributes to the stability of [5-55]. A recombinant model of [5-55], with the remaining Cys residues changed to Ala and a Met residue added to the NH_2-terminus, has a melting temperature (T_m) of ~40°C and contains extensive native structure (*13*). In addition, a peptide model of [5-55] with Cys^{30} and Cys^{51} changed to Ala has a T_m of ~28°C and contains native structure (*11*). A different recombinant model of [5-55], containing the amino acid substitution $Met^{52} \rightarrow$ Arg and the remaining Cys residues changed to Ser, contains native structure that is less stable, unfolding between 10° and 15°C (*12*). Thus, alanine appears to be a better model for protonated thiols than serine since folding experiments at neutral pH (Figs. 8B and 9) indicate that [5-55] is well populated at 25°C, although the Met^{52}

→ Arg substitution may also have a destabilizing effect in the Ser model.

Revision of the BPTI-folding pathway. The folding pathway of BPTI at pH 7.3 is summarized in Fig. 10. Nonnative intermediates are not populated significantly when folding occurs at pH 8.7 (Fig. 5), and are almost absent when folding is observed at neutral pH (Fig. 9). Whereas earlier studies led to the conclusion that eight different disulfide-bonded species were populated substantially in the folding of BPTI, three of them nonnative, only six well-populated disulfide species are seen here, and none of these contain nonnative disulfide bonds (Fig. 10).

Two native intermediates, [30-51] and [5-55], predominate at the single-disulfide stage. Initially, R is oxidized to a large number of mixed disulfide species and single-disulfide intermediates (*19, 29*), which then rearrange rapidly to either [30-51] or [5-55] (Figs. 8 and 9). Both of these intermediates are thought to contain substantial native-like structure (*11–13, 33, 34*). Because the thiols of Cys^{14} and Cys^{38} are solvent exposed in native BPTI (Fig. 1), they can form mixed disulfides in a native-like intermediate without significant loss in energy. Thus, the 14-38 disulfide bond forms readily in both [30-51] and [5-55] to give [30-51; 14-38] and [5-55; 14-38] (that is, N*), respectively.

This leads to a fork in the folding pathway (*2, 11*) (Fig. 10). Both of the resultant two-disulfide intermediates contain extensive native-like structure (*15, 28*). Both intermediates serve as kinetic traps for folding. Since it is very stable, N* does not rearrange further on the time scale of the experiment (Fig. 10).

The intermediate [30-51; 14-38] does rearrange, albeit slowly, to form either N_{SH}^{SH} or N* (Figs. 6A and 10). The prolonged abundance of [30-51; 14-38] together with the observation that urea accelerates the rate of rearrangement (Fig. 6B), suggests strongly that essentially complete native folding of this intermediate (Fig. 7) retards the rate of rearrangement. This retardation is apparent at pH 8.7 (Fig. 5B) but is enhanced substantially at pH 7.3 (Fig. 9), presumably because folded structure in the intermediate is more stable at neutral pH.

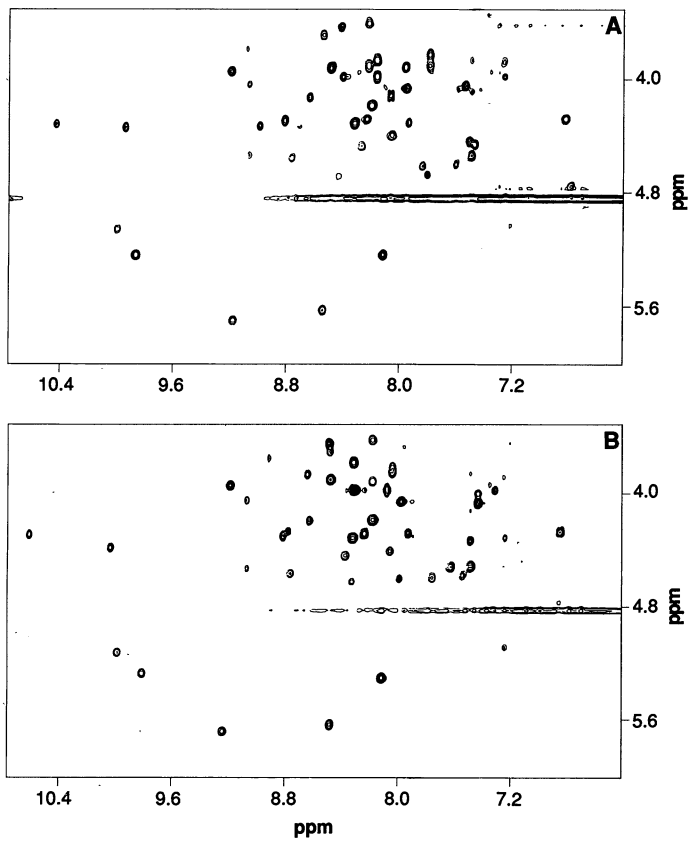

Fig. 7. Comparison of the 2D-NMR TOCSY spectra for: (**A**) Acid-quenched [30-51; 14-38]. (**B**) Native BPTI. The spectra were taken at 20°C, pH 3.6 (*47*). Only the "fingerprint" region, which includes cross peaks between protons on adjacent amides and alpha carbons, is shown.

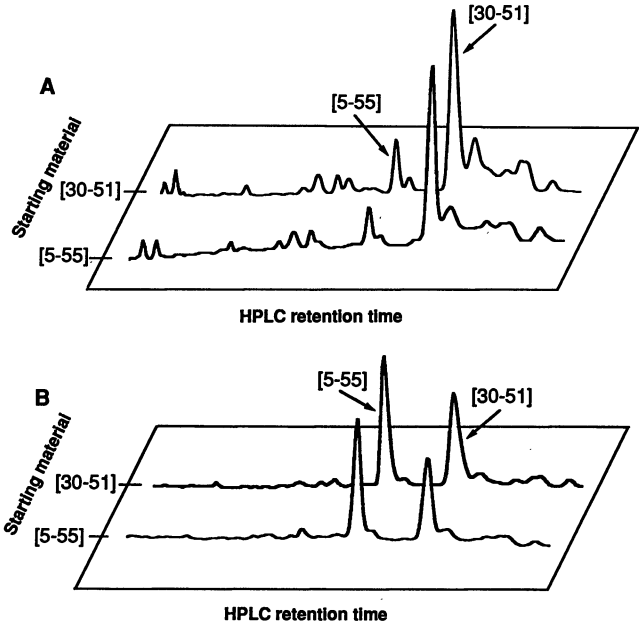

Fig. 8. Equilibrium distribution of single-disulfide intermediates (*45*). As a check that equilibrium had been reached, the rearrangements were started with two different purified intermediates, [30-51] and [5-55]. (**A**) pH 8.7, 25°C; (**B**) pH 7.3, 25°C.

Native folding of [30-51; 14-38] would also bury the thiols of Cys^5 and Cys^{55}, thereby inhibiting the first step in direct oxidation to N (that is, formation of a mixed disulfide with the oxidizing agent). A similar phenomenon has been observed with N* (*2*) and with the constant fragment of the immunoglobulin light chain (*22*). Direct measurement, however, of the reactivity of thiols in [30-51; 14-38] have not yet been made. Other factors, such as the structure of the transition state (*32*), or of the stability of mixed disulfide species that are populated in strongly oxidizing conditions (or bond) could also influence the overall rate of direct oxidation; for example, the presence of a mixed disulfide with glutathione on Cys^5 or Cys^{55} is likely to destabilize or partially unfold the intermediate [30-51; 14-38].

Since only one cysteine in a disulfide bond can be exchanged in a single step, the rearrangement of [30-51; 14-38] to N_{SH}^{SH} or N* must proceed through nonnative intermediates. Although not well populated, two of the nonnative intermediates found earlier, [30-51; 5-14] and [30-51; 5-38], can be detected in the rearrangement experiment (Fig. 6A). More work is needed to evaluate the kinetic importance of these nonnative intermediates. The striking observation, however, is that the rearrangement from [30-51; 14-38] to N* occurs almost as rapidly as the rearrangement to N_{SH}^{SH} (Figs. 6A, 10), even though the rearrangement to N* requires an intermediate that is distinct from [30-51; 5-14] or [30-51; 5-38].

Thus, the rearrangement process appears to be relatively random. There is no evidence that the nonnative intermediates [30-51; 5-14] and [30-51; 5-38] serve to "direct" folding toward N_{SH}^{SH}. Rather, it seems likely that before the third disulfide bond in BPTI can be formed, [30-51; 14-38], like N*, must unfold substantially in order to expose thiols that are buried as a result of native structure (*22, 28*).

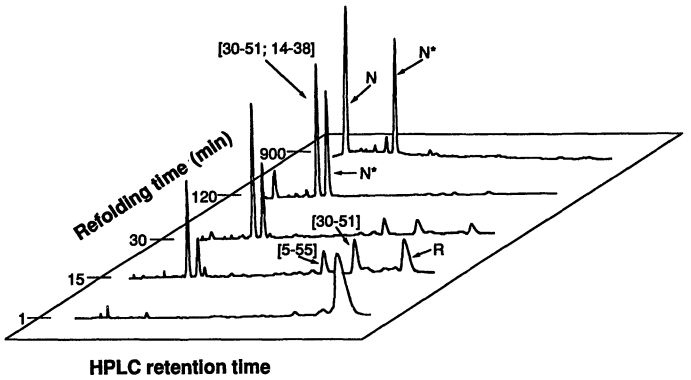

Fig. 9. Folding of BPTI at neutral pH. The experiment is identical to that in Fig. 5B, but at pH 7.3 rather than pH 8.7. N^{SH}_{SH} is not well populated because formation of the 14-38 disulfide is fast (when oxidized 150 μM glutathione is used) compared to the rate of rearrangement of [30-51; 14-38].

It is possible that the need to unfold native structure before the completion of folding is a more general phenomenon. For example, recent experiments suggest that specific native tertiary interactions in a folding intermediate of ribonuclease T1 retard the rate-limiting step in folding by trapping partially folded structure (*31*). In addition, chaperonin proteins (*35*), by preferentially binding the unfolded state in an ATP-dependent manner, may function in part by promoting the unfolding of kinetically trapped folding intermediates.

Implications for the mechanism of protein folding. The cooperative nature of protein folding reactions has made it difficult to find conditions in which folding intermediates are well populated. Despite this difficulty, various techniques are now beginning to provide detailed information about protein folding intermediates (*36, 37*). Three approaches have been particularly productive: (i) measurement of individual NH (amide) proton exchange rates in folding intermediates by NMR (*38, 39*); (ii) building of peptide models corresponding to folding intermediates (*11, 33*); and (iii) trapping of inherently unstable disulfide-bonded intermediates (*1, 2*).

Results from both pulsed amide proton exchange and peptide model studies suggest that folding intermediates contain native-like secondary and tertiary structure. Both methodologies, however, are biased toward the observation of native over nonnative structure. A central assumption in the design of peptide models is that local native interactions stabilize the structure in folding intermediates (*11, 33*). Pulsed amide proton exchange experiments only monitor protons that are well protected in the native protein. Thus, it is possible that nonnative structure would be difficult to detect (*27, 40*).

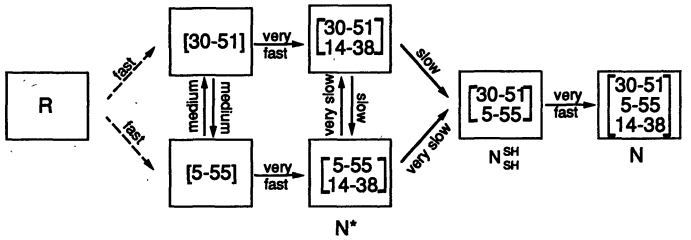

Fig. 10. Schematic of the folding pathway for BPTI. Qualitative estimates of the relative rates of the intramolecular transitions (*48*) associated with each step at pH 7.3 are indicated. These rates range from milliseconds for the "very fast" transitions to months for the "very slow" ones. N* is a kinetically trapped intermediate (*15*). The dotted arrows indicate that R is oxidized initially to a broad distribution of single disulfide intermediates, which then rearranges rapidly to [30-51] and [5-55].

The trapping of disulfide-bonded intermediates makes it possible to view folding intermediates without bias for native structure. Earlier studies, indicating that there are well-populated and persistent intermediates containing nonnative disulfide bonds in the oxidative folding of BPTI, have provided the strongest evidence indicating that nonnative protein interactions are relevant for protein folding.

Our conclusion that there are no well-populated, nonnative intermediates in the folding of BPTI removes a major unresolved problem in many diverse models for protein folding that invoke predominantly native interactions. It seems likely that the same interactions that stabilize the final folded structure also guide the protein in attaining this structure (*41*). To the extent that it is true, this simplifying principle should facilitate both experimental and theoretical efforts toward our understanding of protein folding.

REFERENCES AND NOTES

1. T. E. Creighton, *Prog. Biophys. Mol. Biol.* **33**, 231 (1978).
2. _____ and D. P. Goldenberg, *J. Mol. Biol.* **179**, 497 (1984).
3. Intermediates are denoted in brackets by the disulfide linkage of the Cys residues. Parentheses are used to denote the identity of IEC peaks as determined in (*9*).
4. T. E. Creighton, *J. Mol. Biol.* **113**, 275 (1977).
5. _____, *ibid.* **87**, 563 (1974).
6. J. R. Brown and B. S. Hartley, *Biochem. J.* **101**, 214 (1966).
7. Blocked intermediates were lyophilized after HPLC separation and then reduced with 250 μl of 10 mM dithiothreitol (DTT) (Sigma) in 6 M guanidine-HCl, 100 mM tris-hydroxymethyl-aminomethane hydrochloride (tris-HCl), pH 8.7, 1 mM EDTA. After 2 hours, an equal volume of 100 mM IAEDANS (Molecular Probes) in the same buffer was added to label the free thiols. After 5 minutes the mixture was desalted in 10 mM HCl (PD-10, Pharmacia). The tagged peak was then digested with thermolysin at 65°C for 1.25 hours (75 μg/ml in 100 mM tris-HCl, pH 8.7, 2 mM $CaCl_2$). Digestion was quenched by the addition of EDTA to 5 mM and acetic acid to 5 percent. Peptide fragments were separated by HPLC on a Vydac C-18 analytical column; monitoring absorbance simultaneously at 340 nm, where only IAEDANS-labeled peptides are observed, and at 229 nm, where all peptides are detected. As with all other HPLC separations, an acetonitrile-H_2O gradient in the presence of 0.1 percent trifluoroacetic acid (TFA) was used. For the native standard, peptides were identified by their amino acid sequences. Subsequent identifications were made by comparing elution times to these standards. Acid-quenched intermediates were blocked by resuspending the dried intermediate in a buffer consisting of 500 mM sodium iodoacetate, 100 mM tris-HCl, pH 8.7, 200 mM KCl and 1 mM EDTA for 30 seconds, followed by desalting on a PD-10 column equilibrated in 10 mM HCl and HPLC purification.
8. For example, proteolytic fragments of an intermediate could be separated by HPLC in both the reduced and oxidized form. Fragments that contain disulfide bonds disappear on reduction. These fragments could then be identified by mass spectrometry or amino acid sequencing. Similar identifications have been carried out on other proteins [for example, C. Carr, S. Aykent, N. M. Kimack, A. D. Levine, *Biochemistry* **30**, 1515 (1991)].
9. T. E. Creighton, *J. Mol. Biol.* **95**, 167 (1975).
10. BPTI (FBA pharmaceuticals) was purified in the reduced form on a Vydac C-18 preparative column. Reduced BPTI in 10 mM HCl (*9*) was diluted to a final concentration of 30 μM by the addition of Milli-Q water and a stock (5×) solution of folding buffer (final conditions: 100 mM tris-HCl, pH 8.7, 200 mM KCl, 1 mM EDTA). Folding was initiated by the addition of 100 mM oxidized glutathione (Sigma) to a final concentration of 150 μM. All buffers were degassed and equilibrated at 25°C prior to mixing. Oxidation proceeded in an evacuated chamber with temperature regulated by pumping water from a cooling bath through coils that were submerged in this chamber. All subsequent folding experiments were done as described above, except that 100 mM phosphate buffer was used for the experiments at pH 7.3. Folding was quenched after 3 minutes, at a pH of 8.0, by addition of one-fourth volume of 500 mM sodium iodoacetate (Sigma) in 250 mM tris-HCl, and pH 6.8 buffer. After 2 minutes the quenched folding mix was desalted on a (5.5 × 25 cm) Sephadex G25 (Pharmacia) column equilibrated with 20 mM imidazole-HCl, pH 6.2, 1 mM EDTA, and then loaded directly onto a 1.5 × 75 cm carboxymethyl-cellulose (Sigma) column equilibrated in the same buffer. The intermediates were eluted with a concave NaCl gradient (*9*). IEC peaks were pooled (Fig. 3A) and placed on a Vydac C-18 semipreparative column heated to 45°C. The temperature of the column was reduced to 37°C for the separation of acid-quenched intermediates. The HPLC peaks were analyzed by CZE (Beckman P/ACE or ABI 270) with 50 mM phosphate, pH 2.0, 0.1 percent triethylamine buffer, and monitoring at 200 nm.
11. J. P. Staley and P. S. Kim, *Nature* **344**, 685 (1990).
12. N. J. Darby, C. P. M. van Mierlo, T. E. Creighton, *FEBS Lett.* **279**, 61 (1991).
13. J. P. Staley and P. S. Kim, unpublished 2D-NMR data.
14. [30-51; 5-55], which was shown to have extensive native structure by 2D-NMR studies [C. I. Stassinopoulou, G. Wagner, K. Wüthrich, *Eur. J. Biochem.* **145**, 423 (1984)], is formed rapidly by reducing N with DTT and is resistant to further reduction [T. E. Creighton, *J. Mol. Biol.* **113**, 295 (1977)]. This intermediate is termed N^{SH}_{SH}.

15. [5-55; 14-38], designated N* because of its native-like structure as determined by x-ray crystallography of a recombinant model [C. Eigenbrot, M. Randal, A. A. Kossiakoff, *Protein Eng.* **3**, 591 (1990)], does not oxidize readily to N because the remaining thiols, on cysteines 30 and 51, are buried and thus inaccessible to oxidizing agent (*2, 11*). N* coeluted with native BPTI by IEC (see Fig. 3) and was recognized after NMR studies of refolded BPTI detected a contaminating species [D. J. States *et al.*, *Nature* **286**, 630 (1980)].
16. T. E. Creighton, *J. Mol. Biol.* **87**, 579, 603 (1974).
17. _____, *Methods Enzymol.* **107**, 305 (1984).
18. J. S. Weissman and P. S. Kim, unpublished data.
19. T. E. Creighton, *Biophys. Chem.* **31**, 155 (1988).
20. T.-Y. Lin and P. S. Kim, *Biochemistry* **28**, 5282 (1989).
21. T. E. Creighton, *J. Mol. Biol.* **96**, 777 (1975).
22. Y. Goto and K. Hamaguchi, *ibid.* **146**, 321 (1981).
23. G. H. Snyder *et al.*, *Biochemistry* **20**, 6509 (1981).
24. D. M. Rothwarf and H. A. Scheraga, *J. Am. Chem. Soc.* **113**, 6293 (1991).
25. J. S. Weissman and P. S. Kim, unpublished data. For an example, see the zero time point of Fig. 6A.
26. The rate-limiting step is taken to be the step with the greatest free energy difference between its transition state and the lowest free energy intermediate preceding it [S. Yagisawa, *Biochem. J.* **263**, 985 (1989)].
27. T. E. Creighton, *Biochem. J.* **270**, 1 (1990).
28. J. S. Weissman, Z.-Y. Peng, P. S. Kim, unpublished results. Assignments for native BPTI are given by G. Wagner and K. Wüthrich, *J. Mol. Biol.* **155**, 347 (1982).
29. T. E. Creighton, *J. Mol. Biol.* **113**, 313 (1977).
30. L. F. McCoy, E. S. Rowe, K.-P. Wong, *Biochemistry* **19**, 4738 (1980).
31. T. Kiefhaber, H.-P. Grunert, U. Hahn, F. X. Schmid, *Proteins*, in press.
32. D. P. Goldenberg and T. E. Creighton, *Biopolymers* **24**, 167 (1985).
33. T. G. Oas and P. S. Kim, *Nature* **336**, 42 (1988).
34. D. J. States *et al*, *J. Mol. Biol.* **195**, 731 (1987).
35. For reviews, see: J. E. Rothman, *Cell* **59**, 591 (1989); F. X. Schmid, *Curr. Opinion Struct. Biol.* **1**, 36 (1991).
36. P. S. Kim and R. L. Baldwin, *Annu. Rev. Biochem.* **59**, 631 (1990).
37. T. E. Creighton and P. S. Kim, *Curr. Opinion Struct. Biol.* **1**, 3 (1991).
38. F. X. Schmid and R. L. Baldwin, *J. Mol. Biol.* **135**, 199 (1979); J. B. Udgaonkar and R. L. Baldwin, *Nature* **335**, 694 (1988); H. Roder *et al.*, *ibid.*, p. 700; M. Bycroft *et al.*, *ibid.* **346**, 488 (1990).
39. J. Baum, C. M. Dobson, P. A. Evans, C. Hanley, *Biochemistry* **28**; 7 (1989); F. M. Hughson, P. E. Wright, R. L. Baldwin, *Science* **249**, 1544 (1990); M.-F. Jeng, S. W. Englander, G. A. Elöve, A. J. Wand, H. Roder, *Biochemistry* **29**, 10433 (1990).
40. C. M. Dobson, *Curr. Opinion Struct. Biol.* **1**, 22 (1991).
41. For example, in the subdomain model (*11, 33, 36*) protein folding is viewed as a hierarchical condensation process [G. D. Rose, *J. Mol. Biol.* **134**, 447 (1979)] involving cooperatively folded subdomains of native structure, and the predominant source of cooperativity is native tertiary interactions.
42. A BPTI folding mixture (12 ml) was split into three portions of 4 ml each (*10*). At 5 minutes, folding was quenched by the addition of 1 ml of 0.125, 0.5, or 2 M iodoacetate stock solution (*43*), or by the addition of 50, 200, or 800 μl of formic acid (*44*).
43. Iodoacetate quenching is achieved by the addition of one-fourth volume of a stock (5×) solution of sodium iodoacetate in 250 mM tris-HCl, pH 6.8. After a period inversely proportional to the final concentration of iodoacetate used (1 minute for 400 mM) the protein is desalted on a PD-10 column equilibrated in 10 mM HCl. For the HPLC separations, buffer A is 0.1 percent trifluoroacetic acid (TFA) in water, and buffer B is 0.1 percent TFA, 90 percent acetonitrile, and 10 percent water. The gradient used is 0 minutes, 90 percent A; 15 minutes, 75 percent A; 75 minutes, 72 percent A; 135 minutes, 70 percent A; 155 minutes, 69 percent A.
44. Acid quenching is achieved by the addition of 1/20th volume of 88 percent formic acid, to give a final pH of ~2. When a delay between acid quenching and HPLC analysis was necessary because multiple time points were taken, the experiment was repeated with the order of chromatography altered to demonstrate that rearrangement was not occurring while the mix awaited separation. The gradient used for the HPLC separations is 0 minutes, 90 percent A; 15 minutes, 75 percent A; 35 minutes, 73 percent A; 50 minutes, 72 percent A; 140 minutes, 69 percent A.
45. Acid-quenched intermediates were purified by HPLC and lyophilized. Rearrangement was initiated by the addition of degassed folding buffer. The experiment was carried out in a water bath at 25°C in an anaerobic chamber (Coy Laboratory Products, Ann Arbor, MI). The single disulfides were allowed to rearrange for 2.5 minutes at pH 8.7 or 45 minutes at pH 7.3.
46. The [30-51; 14-38] intermediate was allowed to rearrange in folding buffer containing urea. The appearance of N* and N_{SH}^{SH} was monitored as a function of time and the rate of the sum of these intermediates was fit to an exponential in order to determine the unimolecular rate constant for rearrangement. In the presence of urea, a significant population of intermediates appears transiently, and the rate of formation of N* and N_{SH}^{SH} deviates from a simple exponential. Nevertheless, the data demonstrate that the rate of formation of N* and N_{SH}^{SH} increases substantially upon addition of denaturant.
47. Samples were prepared for NMR (Bruker 500 MHz spectrometer) by adding lyophilized protein to Milli-Q water 10 percent D_2O containing 20 μM EDTA and the pH was adjusted with NaOH. HPLC analysis indicated that less than 10 percent of the [30-51; 14-38] had rearranged or oxidized during the data collection.
48. J. S. Weissman and P. S. Kim, in preparation. The rate of oxidation with cyclic oxidizing agents like DTT is proportional to the rate of the intramolecular process that brings the cysteine thiols together. This makes it possible to compare steps in folding that involve intermolecular disulfide bond formation to those that involve only intramolecular thiol-disulfide exchange (*17*).
49. We thank J. P. Staley for helpful discussions; R. L. Baldwin and D. P. Goldenberg for helpful comments on earlier drafts of this manuscript; and Z.-Y. Peng for assistance with NMR measurements. Supported by the Karl Taylor Compton and NSF predoctoral fellowship programs (J.S.W.) and by grants from the NIH (GM 41307 and RR 05927), the Pew Memorial Trust, and the Rita Allen Foundation.

24 April 1990; accepted 9 August 1990

(*continued from page 1367*)

tween bases 60 and 70 were not well protected by TFIIIA, a result consistent with finger 6 behaving differently compared to the other fingers. Hydroxyl radical footprinting of finger deletion mutants of TFIIIA is consistent with the placement of fingers 1-2 and 8-9 as was shown (*12*).

The less regular mode of binding hypothesized for TFIIIA relative to the Zif268 structure may arise from irregularities in some of the TFIIIA zinc fingers. Fingers 3, 6, and 8 have His-X_4-His spacings between the histidine ligands instead of the more prevalent His-X_3-His spacing. The His-X_4-His fingers have more conformational flexibility than the His-X_3-His fingers (*13, 14*). Also, the linker length between fingers may influence the precise mode of binding (number of residues between the last His and first Cys in neighboring fingers). In the proposed model, the three subsites are spanned by His-X_4-His fingers with irregular linker lengths. These variations on the more regular His-X_3-His domain may serve to increase and diversify the binding sites available to multifinger proteins.

How general, then, is the recognition pattern of a single protein-DNA complex? Structures of the helix-turn-helix motif suggest that if there is a pattern, it will be more complex than the scheme outlined here. However, a scheme for making predictions that can be tested experimentally, both by structural analysis and by site-directed mutagenesis, should yield some insights into the nature of this class of zinc finger–DNA recognition.

REFERENCES AND NOTES

1. J. Miller, A. D. McLachlan, A. Klug, *EMBO J.* **4**, 1609 (1985).
2. R. S. Brown, C. Sander, P. Argos, *FEBS Lett.* **186**, 271 (1985).
3. G. Párraga *et al.*, *Science* **241**, 1489 (1988).
4. M. S. Lee, G. P. Gippert, K. V. Soman, D. A. Case, P. E. Wright, *ibid.* **245**, 635 (1989).
5. R. E. Klevit, J. R. Herriott, S. J. Horvath, *Proteins: Struct. Funct. Genet.* **7**, 215 (1990).
6. J. G. Omichinski, G. M. Clore, E. Appella, K. Sakaguchi, A. M. Gronenborn, *Biochemistry* **29**, 9324 (1990).
7. N. P. Pavletich and C. O. Pabo, *Science* **252**, 809 (1991).
8. J. Nardelli, T. J. Gibson, C. Vesque, P. Charnay, *Nature* **349**, 175 (1991).
9. N. C. Seeman, J. M. Rosenberg, A. Rich, *Proc. Natl. Acad. Sci. U.S.A.* **73**, 804 (1976).
10. K. Nagai, Y. Nakaseko, K. Nasmyth, D. Rhodes, *Nature* **332**, 284 (1988).
11. S. Thukral, A. Eisen, E. T. Young, *Mol. Cell. Biol.* **11**, 1566 (1991).
12. L. Fairall, D. Rhodes, A. J. Klug, *J. Mol. Biol.* **192**, 577 (1986).
13. R. X. Xu, S. J. Horvath, R. E. Klevit, *Biochemistry* **30**, 3365 (1991).
14. M. Kochoyan *et al.*, *ibid.*, p. 3371.